④

GL-TR-89-0304
ENVIRONMENTAL RESEARCH PAPERS, NO. 1046

Wind Field Derivatives of Extratropical Cyclones
Observed by Doppler Radar

AD-A222 188

FRANK H. RUGGIERO

6 November 1989

DTIC
ELECTE
JUNO 4 1990
S B D
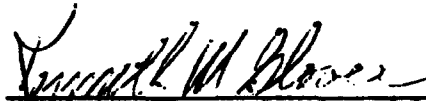
ATMOSPHERIC SCIENCES DIVISION   PROJECT 2781
GEOPHYSICS LABORATORY
HANSCOM AFB, MA 01731-5000

99 05 31 069

"This technical report has been reviewed and is approved for publication"

FOR THE COMMANDER

KENNETH M. GLOVER, Chief
Ground Based Remote Sensing Branch
Atmospheric Sciences Division

ROBERT A. McCLATCHEY, Director
Atmospheric Sciences Division

REPORT DOCUMENTATION PAGE

Form Approved
OMB No. 0704-0188

1a. REPORT SECURITY CLASSIFICATION	1b. RESTRICTIVE MARKINGS
Unclassified	

2a. SECURITY CLASSIFICATION AUTHORITY	3. DISTRIBUTION / AVAILABILITY OF REPORT
	Approved for public release;
2b. DECLASSIFICATION / DOWNGRADING SCHEDULE	distribution unlimited.

4. PERFORMING ORGANIZATION REPORT NUMBER(S)	5. MONITORING ORGANIZATION REPORT NUMBER(S)
GL-TR-89-0304 ERP, No. 1046	

6a. NAME OF PERFORMING ORGANIZATION	6b. OFFICE SYMBOL (If applicable)	7a. NAME OF MONITORING ORGANIZATION
Atmospheric Sciences Division Geophysics Laboratory	GL/LYR	

6c. ADDRESS (City, State, and ZIP Code)	7b. ADDRESS (City, State, and ZIP Code)
Hanscom AFB Massachusetts 01731-5000	

8a. NAME OF FUNDING / SPONSORING ORGANIZATION	8b. OFFICE SYMBOL (If applicable)	9. PROCUREMENT INSTRUMENT IDENTIFICATION NUMBER

8c. ADDRESS (City, State, and ZIP Code)	10. SOURCE OF FUNDING NUMBERS			
	PROGRAM ELEMENT NO.	PROJECT NO.	TASK NO.	WORK UNIT ACCESSION NO.
	63707F	2781	01	03

11. TITLE (Include Security Classification)

Wind Field Derivatives of Extratropical Cyclones Observed by Doppler Radar

12. PERSONAL AUTHOR(S)
Ruggiero, F.H.

13a. TYPE OF REPORT	13b. TIME COVERED	14. DATE OF REPORT (Year, Month, Day)	15. PAGE COUNT
Final	FROM _____ TO _____	1989 November 6	34

16. SUPPLEMENTARY NOTATION

17. COSATI CODES			18. SUBJECT TERMS (Continue on reverse if necessary and identify by block number)
FIELD	GROUP	SUB-GROUP	Extratropical cyclones, Doppler radar, Wind field derivatives

19. ABSTRACT (Continue on reverse if necessary and identify by block number)

A technique to extract wind field derivatives and storm characteristic indices from data acquired by a single Doppler radar is described. The technique was applied to four extratropical cyclones observed in Massachusetts. Storm intensity indices that have worked well in tropical cyclones did not perform as well with the extratropical cyclones. The differences of structure between extratropical and tropical cyclones is mainly responsible for the poor performance of the indices. It is possible that when a network of Doppler radars is deployed a comparative analysis of the wind field derivatives and their indices would provide useful forecasting information.

20. DISTRIBUTION/AVAILABILITY OF ABSTRACT	21. ABSTRACT SECURITY CLASSIFICATION
☒ UNCLASSIFIED/UNLIMITED ☐ SAME AS RPT. ☐ DTIC USERS	Unclassified

22a. NAME OF RESPONSIBLE INDIVIDUAL	22b. TELEPHONE (Include Area Code)	22c. OFFICE SYMBOL
Frank H. Ruggiero	617-377-3646	LYR

DD FORM 1473, JUN 86   *Previous editions are obsolete.*   SECURITY CLASSIFICATION OF THIS PAGE

Preface

The author would like to thank Mr. Ralph J. Donaldson, Jr. and Dr. F. Ian Harris for their advice and suggestions made in preparation of this report. In addition the author would like to express his gratitude to the engineering and technical staff at the GL Ground Based Remote Sensing Branch, in particular Mr. Graham Armstrong, Mr Alexander Bishop, Mr. William Smith, and TSgt Richard Chanley. These men did an outstanding job of operating and maintaining the GL radar, often in extremely inclement weather, to help make this work possible.

iii

Contents

Illustrations

Tables

Wind Field Derivatives of Extratropical Cyclones Observed by Doppler Radar

1. INTRODUCTION

Donaldson and Harris[1] began a new chapter in the analysis of single Doppler velocity radar data by their attempt to go beyond the assumption of a linear wind field. This was done by using information on modeled curved wind fields as well as linear wind fields with speed gradients. They applied their newly found technique to reinterpret data observed from Hurricane Belle in 1976. The application of the technique was subsequently improved and used to estimate the four first order wind field derivatives, namely, downwind shear, diffluence, curvature, and crosswind shear. The technique was tested on data from Hurricane Gloria (Donaldson and Ruggiero[2] and Ruggiero and Donaldson[3]) resulting in the development of the Storm Strength Index (SSI). The SSI is based on the asymmetry found in the Velocity-Azimuth Display (VAD) and can be used to measure the intensity of a tropical cyclone using a fixed position Doppler radar. The SSI is relatively independent of the storm's location

1. Donaldson, R.J., Jr. and Harris, F.I. (1984) Detection of wind field curvature and wind speed gradients by a single Doppler radar, *Preprints, 22nd Conf. Radar Meteorol.*, Am. Meteorol. Soc., Boston, pp. 514-519.

2. Donaldson, R.J., Jr. and Ruggiero, F.H. (1986) Wind field derivatives in Hurricane Gloria estimated by Doppler radar, *Preprints, 23rd Conf. Radar Meteorol.*, Am. Meteorol. Soc., Boston, pp. 236-239.

3. Ruggiero, F.H. and Donaldson, R.J., Jr. (1987) Wind field derivatives: A new diagnostic tool for analysis of hurricanes by a single Doppler radar, *Preprints, 17th Conf. Hurricanes and Tropical Meteorol.*, Am. Meteorol. Soc., Boston, pp. 178-181.

with respect to the radar. Donaldson[4] developed another index called Potential Vortex Fit (PVF). The index of PVF quantifies how close the flow within the VAD circle approximates a potential vortex regime. Both indices are seen as possible Next Generation Weather Radar (NEXRAD) tropical cyclone algorithms because in Hurricane Gloria the SSI and PVF accurately revealed the decay of the storm while it was still 200 km from the radar even though winds near the radar site were still increasing.

While the application of the wind field derivative technique to Hurricane Gloria produced useful results, it is hard to make a case for a NEXRAD algorithm on the basis of one intensively analyzed storm. Obviously, the next logical step is to analyze data from other tropical cyclones. However, the only presently available observations by land based Doppler radar of tropical cyclones occurring in the United States that were not already significantly decayed by the time of observation are the aforementioned Hurricanes Belle and Gloria. An alternative was to apply the technique to intense extratropical cyclones that occur along the eastern Atlantic coast during the winter and spring. These storms on occasion produce Doppler velocity signatures similar to those of tropical cyclones.

Extratropical cyclones in their own right have been known for their sometime unpredictablity (Bosart[5]) and damage that they can cause (U.S. Dept of Commerce[6]). These storms present a forecast problem to which there is presently no acceptable solution due to the lack of in-situ observations over the ocean. Radar provides an instrument that is uniquely suited to the observation of extratropical cyclones over coastal waters because of its ability to scan hundreds of kilometers away from its site. With NEXRAD soon to begin deployment exploring the capabilities of the Doppler radar for the diagnosis of extratropical cyclones would seem to be a proper step.

The analysis technique has been applied to several extratropical cyclones that have been observed by the GL S-Band Doppler radar located at Sudbury, MA. The purposes of this study were to determine how the evaluations of the wind field derivatives could be used for better understanding and forecasting extratropical cyclones. In addition we wanted to evaluate the technique itself to see how it holds up under a larger number of cases so that we may improve its application for tropical cyclones.

2. DESCRIPTION OF THE TECHNIQUE

2.1 Theory

The reader interested in a detailed theoretical background of estimating wind field derivatives from observations by a single Doppler radar should refer to Donaldson and Harris.[7] The discussion here will concentrate on the application of the technique to actual data. The first step to estimating the wind field derivatives is to obtain an array of equally spaced radial velocity values for azimuths at

4.   Donaldson, R.J., Jr. (1989) Potential-vortex fit, *Preprints, 24th Conf. Radar Meteorol.*, Am. Meteorol. Soc., Boston.

5.   Bosart, L.F. (1981) The Presidents' Day snowstorm of 18-19 February 1989: A subsynoptic-scale event, *Mon. Wea. Rev.* **109**:1542-1566.

6.   U.S. Dept of Commerce (1984) *Storm Data*, NOAA, NESDIS, NCDC, Asheville, NC, 20 No. 2 (April) p. 4.

7.   Donaldson, R.J., Jr. and Harris, F.I. (1989) On the determination of curvature, diffluence, and shear by Doppler radar, *J. Atmos. and Oceanic Tech.* **6**:26-35.

a constant range and elevation angle. It is best to use relatively low elevation angles so that horizontal wind computations are not affected by the fall speed of the precipitation particles. If one wanted to look at higher elevation angles it may be possible to account for vertical velocity by trying to correlate reflectivity values at a particular location with fall speed. For the present analysis however, it was decided to use elevation angles less than 1.5° which results in the vertical component of less than 0.1 percent of the total observed Doppler radial velocity. As for range, the longer the range the better, to minimize the effect of small perturbations of velocity along the VAD circle. However, it is much more difficult to get a VAD circle with data at all azimuths when the radius of the scanning circle is large. The range of 40 km was selected as a tradeoff between the two limits and to be consistent with previous work.

From the velocity arrays the zeroth, first, and second order Fourier coefficients of the Doppler Velocity-Azimuth Display (VAD) circle are obtained using the following formulas:

$$a_i = \frac{1}{(n/2)} \sum_{\alpha=1}^{n} V_d(\alpha)\cos(i\alpha) \tag{1}$$

$$b_i = \frac{1}{(n/2)} \sum_{\alpha=1}^{n} V_d(\alpha)\sin(i\alpha) \tag{2}$$

where a_i and b_i are the ith order Fourier coefficients, n is the number of Doppler observations, and α is the azimuth angle. To calculate the wind field derivatives it is desirable to have a_1 as close to zero as possible, so that b_1 yields the best estimate of the mean wind speed about the radar scanning circle. This condition is achieved by reorienting the velocity field so that the wind is oriented in the direction of 90°. To accomplish this the actual wind direction must be found, using one of the following equations:

$$\theta = 90° - \tan^{-1}(a_1/b_1) \qquad (\text{if } b_1 > 0) \tag{3a}$$

$$\theta = 270° - \tan^{-1}(a_1/b_1) \qquad (\text{if } b_1 < 0) \tag{3b}$$

where θ is the azimuth of wind direction. Then the azimuth correction is calculated:

$$\phi = \theta - 90 \tag{4}$$

and all the azimuths in the VAD scanning circle are recalculated by:

$$\alpha' = \alpha + \phi \tag{5}$$

From the reoriented data the zeroth, first, and second order Fourier coefficients are recalculated and used to estimate the wind field derivatives:

$$d = (a_0 - 2a_2)/2b_1 \tag{6}$$

$$r/F = (a_0 + 2a_2)2b_1 \tag{7}$$

$$\tilde{c} = 2b_2/b_1 - r/R \tag{8}$$

Downwind shear is represented by d, (r/F) is a representation of diffluence where F is the distance upstream from a fictional streamline apex, $\tilde{c}$ represents normative crosswind shear with r being the radius of the radar scanning circle and R being the distance from the radar site to the circulation center of the storm. Normative crosswind shear is not the actual crosswind shear because it relies on a simple model of the wind field in the vicinity of the storm which essentially states that the curvature of the wind field is inversely proportional to the distance from the storm center. Although the normative crosswind shear may not be an accurate parametrization of the crosswind shear it does give an indication of the relative strength of a storm, since it is based on how close the curvature is to being ideal in the 40 km radius circle about the radar plus the effect of any associated crosswind shear. Normative crosswind shear provided the basis for the SSI which is simply the normative crosswind shear multiplied by b_1/r to give it the dimensions of inverse seconds. As mentioned earlier, promising results were obtained by this method from Hurricane Gloria (Ruggiero and Donaldson[3]).

The best estimate of wind speed is generally the geometric mean of the first-order Fourier coefficient, b_1 and the mean magnitude, V_m of the maximum and minimum values of Doppler velocity in the VAD pattern:

$$V_o(\text{estimate}) = (b_1 V_m)^{1/2} = [b_1(V_{max} - V_{min})/2]^{1/2})$$ (9)

Donaldson[4] has come up with another indicator of storm intensity that he calls Potential Vortex Fit (PVF). Essentially it indicates how closely the observed flow resembles a potential vortex flow.

$$PVF = b_2 R/b_1 r$$ (10)

Donaldson states that a PVF value of 1 indicates that the flow approximates a potential vortex flow regime with the wind speed doubling at half the distance to the circulation center. A value of PVF between 1.0 and 0.5 indicates that there is either a breakdown of the circulation or crosswind shear about the storm. A value of PVF less than 0.5 indicates that there is both a breakdown of the circulation and crosswind shear about the storm.

2.2 Correction for Missing Data

Calculation of the Fourier coefficients requires data at all azimuth angles. Any gaps are filled by a polynomial interpolation scheme that fits the available data to a second order Fourier series function. A second order series is used because the second order Fourier coefficient is the highest order we would want to calculate, since we are not interested in any smaller perturbations of the data. A polynomial interpolation, instead of a simple linear interpolation, is necessary because the data at the edges of a data gap are associated usually with weaker echoes and therefore noisy. The details about the interpolation scheme used are given in Appendix A.

It is difficult to determine how much interpolated data can be used for the actual Fourier computations before unacceptable errors are introduced into the results. The more interpolation that can be done in each case, the more cases can be used. This would help increase the lead time of forecasting the intensity trends of a storm. In the analysis of Hurricane Gloria a subjective method of observing the polynomial interpolation closeness to the actual data was used to decide which cases Fourier analysis would be conducted on. This is not a suitable method since it says nothing at all about how closely the interpolated data approximates the missing data. For this study it was decided

4

to quantify how many interpolated data points can be allowed. In the study, two cases for which the entire velocity array contained actual data were run several times with different amounts of data deleted and therefore having to be ._terpolated. The idea was to see how much real data could be taken away and without adversely affecting the values of the Fourier coefficients. Groups of four different sized gaps were created in order to simulate real data gaps. These gaps were located in the areas of maximum and minimum velocity and near the zero crossings of the velocity array to test the sensitivity of the results to the location of the data gaps.

The cases selected were 27 September 1985 (Hurricane Gloria) 1521 GMT, 1.0 degree elevation angle and 12 February 1988 1603 GMT, 0.5 degree elevation angle. The results are shown in Tables 1 and 2. It can be seen that even small amounts of missing data can adversely affect the results although

Table 1. Percentage change of calculated Fourier coefficients from all the actual data available to some data converted to missing and polynomial interpolation used to fill the gaps. From the case of 27 September 1985, 1621 GMT, 1.0° elevation.

No. Missing Out of 404 Radials Interpolated	Fourier Coefficents			
	a_0	a_2	b_1	b_2
10	5.7	2.0	0.3	0.6
20	9.5	3.4	0.5	0.9
30	13.8	4.7	0.7	1.0
40	7.9	5.7	0.8	1.4

Table 2. Percentage change of calculated Fourier coefficients from all the actual data available to some data converted to missing and polynomial interpolation used to fill the gaps. From the case of 12 February 1988, 1603 GMT, 0.5° elevation.

No. Missing Out of 394 Radials Interpolated	Fourier coefficients			
	a_0	a_2	b_1	b_2
10	30.3	1.8	0.3	4.2
20	52.4	3.8	0.5	6.6
30	67.3	6.2	0.7	9.1
40	92.3	7.9	0.5	11.2

some of the coefficients seem more stable than others. The main reason why b_1 estimations are more robust than a_0 is that the absolute value of b_1 is higher and therefore less susceptible to small variations in the source data.   These results can explain some of the instability in the estimation of the wind field derivatives from Hurricane Gloria presented by Ruggiero and Donaldson.[3] The estimations of downwind shear and diffluence, which use a_0 in their computations fluctuate more than the estimations of crosswind shear and wind speed except for crosswind shear at 1500 meters altitude. It is fortunate that b_1 and, to a lesser extent, b_2 tend to be more stable, since the index SSI is derived from them.

Tables 3 and 4 show the effect on the Fourier coefficients of gaps in actual data in particular

Table 3. Percentage change of calculated Fourier coefficients from data from all 392 radials available to 20 radials missing at a particular point of the velocity array. From the case of 27 September 1985, 1121 EST.

	LOCATION OF GAP OF MISSING DATA			
Fourier Coefficient	Inbound Maximum	Outbound Maximum	Right Zero Doppler	Left Zero Doppler
a	28.0	1.3	2.7	9.0
a_2	10.4	0.5	1.1	2.7
b_1	1.6	0.1	0.0	0.0
b_2	0.9	0.3	0.5	0.9

Table 4. Percentage change of calculated Fourier coefficients from data from all 404 radials available to 20 radials missing at a particular point of the velocity array. From the case of 12 February 1988, 1603 GMT, elevation = 0.5°.

	LOCATION OF GAP OF MISSING DATA			
Fourier Coefficient	Inbound Maximum	Outbound Maximum	Right Zero Doppler	Left Zero Doppler
a	123.5	45.2	4.5	19.2
a_2	5.8	5.6	1.9	9.0
b_1	0.8	0.7	0.1	0.0
b_2	14.7	2.8	0.8	3.0

areas of the velocity array. The most notable overall effect on the coefficients occurs when the interpolated data are near the maximum inbound velocity. This area has the highest absolute values and therefore contributes more to b_1 than the outbound maximum. We would expect the gaps near the two zero crossings to degrade our calculations since the values of velocity change more as a function of azimuth at these locations than at the peaks in amplitude of the functions. However, the interpolation scheme needs to accurately identify the position of the peaks in order to describe the function accurately. The a_0 is the most sensitive of the coefficients to any gaps, regardless of their location.

It is obvious from the above studies that some of the coefficients and the wind field derivatives are very sensitive to relatively small data gaps in the velocity array. In order to process a large number of velocity arrays in the case studies (Section 3) it was decided to apply rather strict requirements to data used for calculations rather than to subjectively determine if the interpolation is close enough to the actual data. Thus the velocity arrays used in this study have no more than 1 percent interpolated data.

6

2.3 Angular Resolution of Data

Another important aspect of employing the technique is the angular resolution needed to produce reliable results. In their work extracting Fourier coefficients from Doppler velocity data, Browning and Wexler[8] used an increment of 10°. We attempted to determine what would be a necessary resolution of data to get reasonably accurate results. The cases cited in Section 2.2 were used. First, data from every other radial were deleted and Fourier calculations were made on the remainder of the data with no interpolation. The procedure was repeated using every third radial for the computations and continued until we were using every 11th radial which roughly corresponded to about 10° of azimuthal resolution. The results are shown in Tables 5 and 6. As with the previous tests there was significant variability between different coefficients in the same cases and between the same coefficients in different cases. The coefficient b_1 calculation is the least affected while a_0 is the most affected.

For most of the case studies in Section 3, the angular resolution of the data was approximately 0.9°. Based on the results just described it was decided to use an angular resolution of 1 degree. It was not desirable to use the angular resolution of the actual data since it was not constant. The values for each degree of azimuth were calculated by linear interpolation of the two velocity values on either side of the particular degree.

3. CASE STUDIES

The data archives of the GL Weather Radar Facility were examined to identify possible cases for the analysis of wind field derivatives. Seven storms, all of which occurred during the Boston Area NEXRAD Demostration (BAND) (Forsyth et al,[9])were chosen for further review. After review of the archive tapes from each of the storms, three cases were rejected due to insufficient velocity data in the 40 km scanning circle to perform the calculations. During the course of this study an intense winter storm that passed near the GL radar site was added to the list of case studies.

3.1 16 November 1983

The storm of 16 November 1983 originated as a deep surface storm centered in Illinois on 15 November. As this system advanced slowly eastward it developed a secondary center over New Jersey by early on 16 November. The associated upper level 500 mb trough over Illinois on 15 November intensified as it advanced slowly eastward and developed a closed circulation over New York on 16 November. The strong southerly flow associated with this system produced heavy rain within radar range throughout the early morning hours on 16 November. The velocity data at 0.5° elevation was sufficient to allow wind field derivative analysis from 0835 to 1356 GMT at the

8. Browning, K.A. and Wexler, R. (1968) The determination of kinematic properties of a wind field using Doppler radar, *J. Appl. Meteorol.* 7:105-113.

9. Forsyth, D.E., Istok, M.J., O'Bannon, T.D., and Glover, K.M. (1985) *The Boston Area NEXRAD Demonstration (BAND)*, AFGL-TR-85-0098, ADA164426.

Table 5. Percentage change of calculated Fourier coefficients from data from all 404 radials available to every nth radial used for the calculations. From the case of 27 September 1985, 1621 GMT, 1.0° elevation.

Number of Radials	Fourier Coefficients			
	a_0	a_2	b_1	b_2
202	8.2	0.2	0.1	5.5
134	2.2	0.5	0.5	2.4
100	23.2	1.6	0.8	22.5
80	6.9	2.0	0.6	15.2
66	59.7	2.0	0.9	32.8
57	12.9	6.1	0.4	13.4
49	3.5	1.4	1.4	61.2
44	4.7	2.7	1.5	35.4
39	82.7	7.6	2.2	83.7
35	96.0	14.4	1.1	105.1

Table 6. Percentage change of calculated Fourier coefficients from when data from all 392 radials were available to when every nth radial was used for the calucations. From the case of 12 February 1988, 1603 GMT, 0.5° elevation.

Number of Radials	Fourier Coefficients			
	a_0	a_2	b_1	b_2
196	0.9	2.2	0.4	3.7
130	79.5	5.5	0.2	13.0
97	120.2	9.8	0.0	12.1
78	54.1	5.1	1.0	21.4
64	171.0	9.2	0.3	41.1
55	21.4	21.8	0.4	7.6
48	277.1	4.3	1.2	44.2
42	358.7	11.7	0.4	45.9
38	40.7	26.8	0.4	26.9
34	419.6	25.7	0.1	44.3

scanning circle radius of 40 km.

Calculations of Storm Strength Index (SSI) and Potential Vortex Fit (PVF) were used to evaluate the coastal low center. However, at 1500 GMT the surface analysis (Figure 1) indicated that at the surface the low center was poorly defined; three low pressure centers were shown. At first it was decided to use the deepest low pressure center to evaluate the indices. The result is shown in Figure 2. The values of PVF in particular are greater than unity, which is abnormally high. Donaldson[4] states
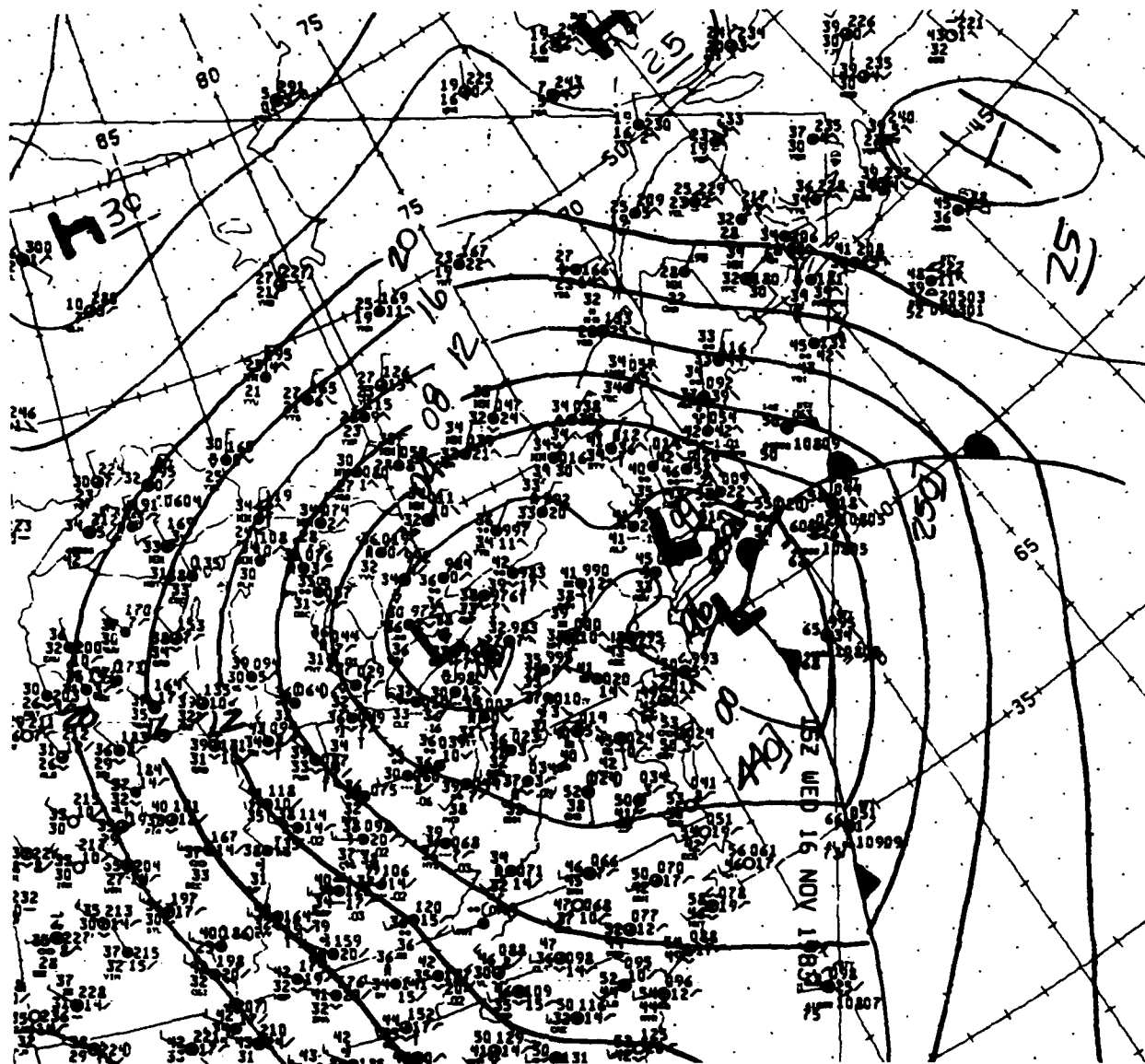
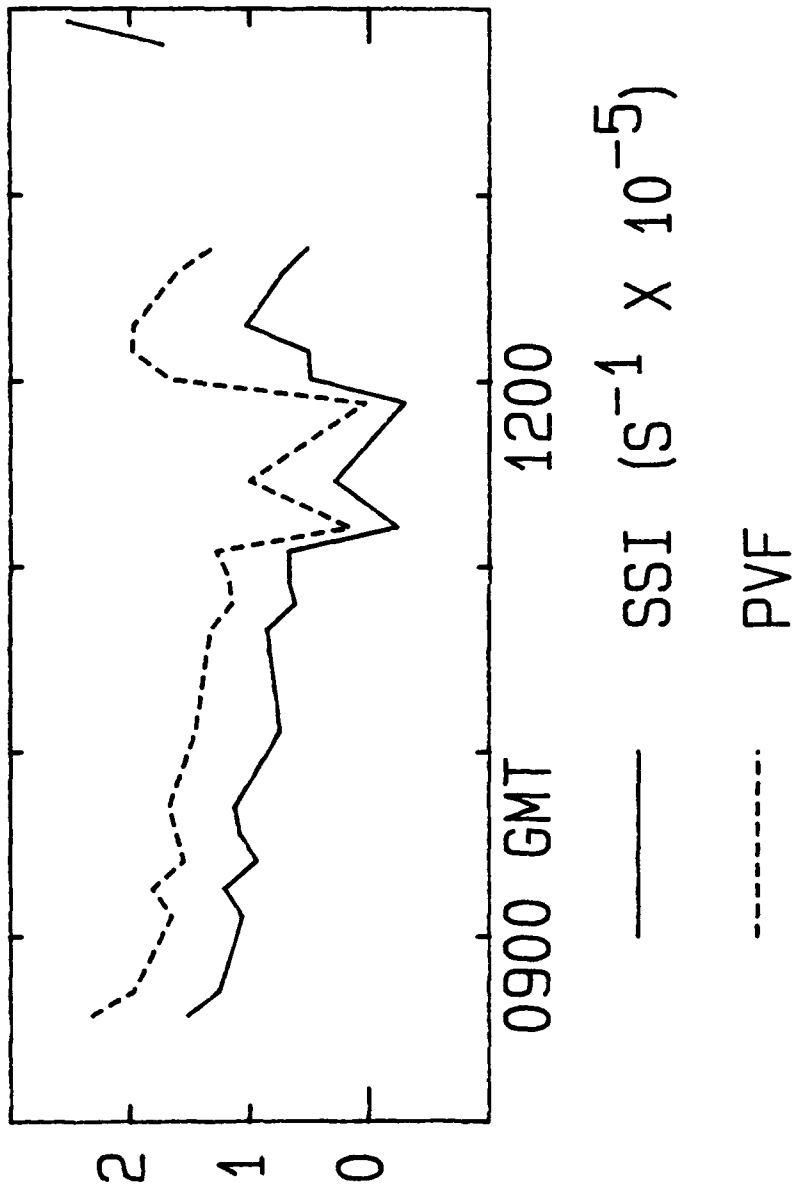Figure 1. Surface Analysis at 1500 GMT 16 November 1983

Figure 2. Values of Storm Strength Index (SSI) and Potential-Vortex Fit During the Passage of the Extratropical Storm on 16 November 1983. Measurement by the GL radar in Sudbury, MA, using the low centered south of Long Island at 1500 GMT for curvature estimation.

that values of PVF greater than one indicate that some influence other than the low center under evaluation must be affecting the data in the VAD circle. In this case the other influence is probably the low pressure center analyzed in northwestern Connecticut. The PVF and SSI were recalculated in relation to the center in Connecticut. The revised estimations are presented in Figure 3. The differences in the PVF values occur after 1200 GMT. The PVF estimates in the revised area appear to be more sensible since they are below one with the exception of the last two estimates at 1349 and 1356 GMT.

The wind speed (Figure 4) as measured within the VAD scanning circle appears to be decreasing as the low appoaches, hence indicating negative crosswind shear. It is surprising that the SSI is not negative. Our parameterization of r/R must be overestimating the actual effect of curvature on the wind field. The estimates of diffluence and downwind shear are presented in Figure 5. For the most part the two derivatives are opposite in sign as one would expect with purely horizontal flow.

3.2 11 January 1984

On 10 January 1984 at 1000 GMT a small weakening storm center was located over north central Pennsylvania and southwestern New York state. At the same time another coastal storm system was rapidly forming off the Carolina coast and eventually led to moderate and heavy snow at and around the radar site. By 1000 GMT 11 January the storm center was rapidly advancing northeastward and was centered just south of the Nantucket Light Ship Buoy. Data were collected by the GL radar from 0208 GMT 11 January until 1311 GMT. The data were sufficient for wind field derivative analysis from 0214 to 0504 GMT and from 0619 to 0806 GMT.

Figure 6 contains the values of downwind shear and diffluence as a function of time during the storm passage. Initially there was positive downwind shear and confluence until about 0319 GMT. Negative downwind shear and diffluence persisted until at least 0504 GMT. Beginning at 0619 GMT and lasting to 0806 GMT there was positive downwind shear and diffluence. These indicate the effect of non-horizontal flow, which is expected in extratropical cyclones.

The data from the second elevation step were used because of gaps of data at the lowest elevation angle. At an elevation angle of 1.4° and a range of 40 km, the height at which the measurements were made was 1182 meters, which is approximately the height of the 850 mb level. To calculate PVF and SSI, the low center at 850 mb between 0000 and 1200 GMT was used to estimate the circulation center. At those times the low center was located approximately 1500 km southwest of the site. The SSI and PVF plots are given in Figure 7. The values of SSI go from positive to negative during the passage of the storm. With only one meter difference in height of the low center between 0000 GMT and 1200 GMT the storm is unlikely to have undergone any serious weakening as the SSI might have indicated. The most probable explanation for this situation is that the low pressure center at 850 mb is so far away that its circulation did not exert a significant impact on the information obtained by the radar. The PVF values follow the same pattern and include some absurdly high values in the beginning and negative values later. This suggests that the circulation near the radar site was being influenced by something other than the 850 mb low to the southwest. Examining the 850 mb analysis (Figure 8) it can be seen that some anticyclonic influence from the ridge moving in from the west is probably causing the negative values of PVF.
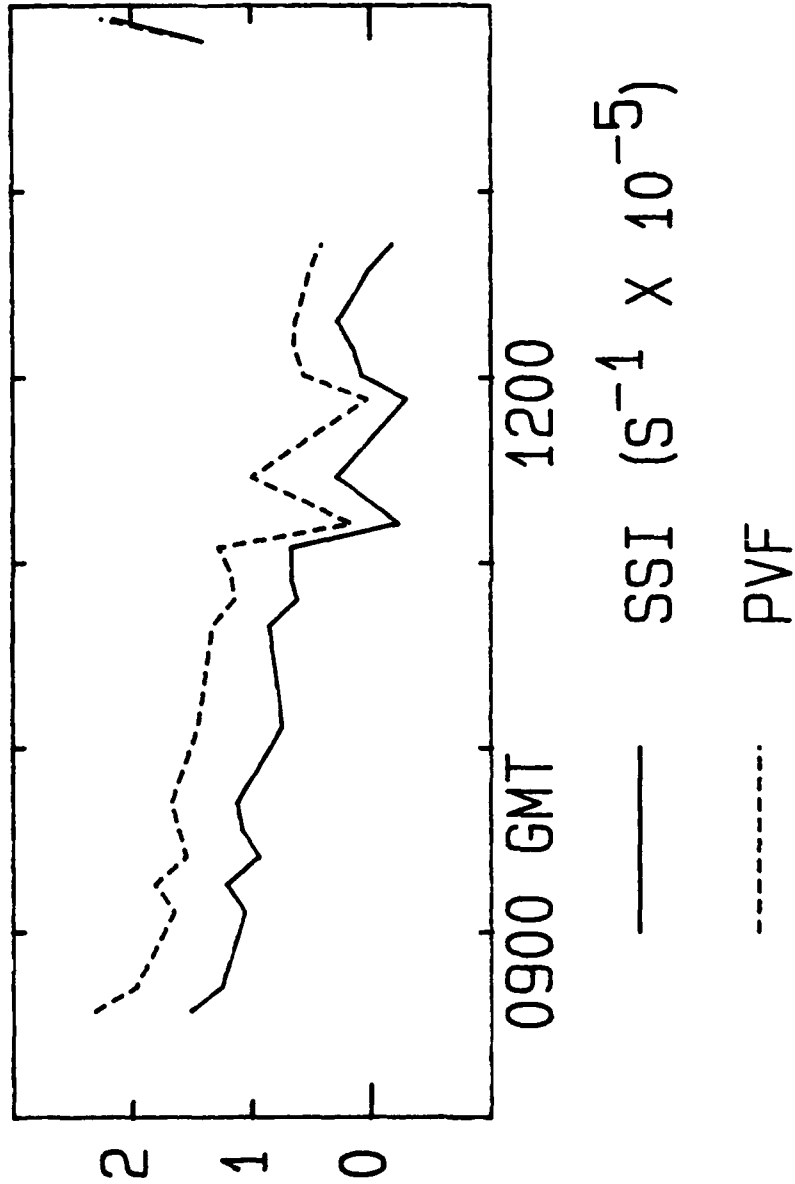
11

Figure 3. Values of Storm Strength Index (SSI) and Potential-Vortex Fit During the Passage of the Extratropical Storm on 16 November 1983. Measurement by the GL radar in Sudbury, MA, using the low centered over western New England at 1500 GMT for curvature estimation.
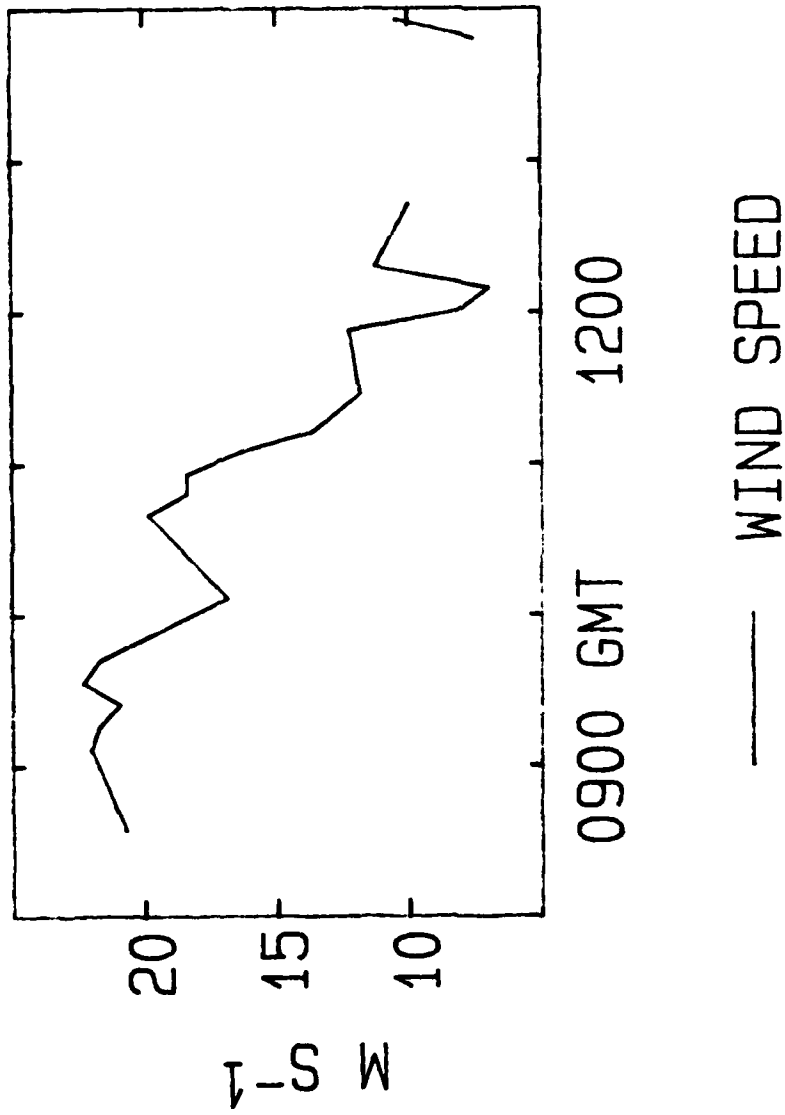
Figure 4. Near Surface Wind Speed Estimations During Passage of the Extratropical Storm on 16 November 1983. Measurement by the GL radar in Sudbury, MA using $(b_1 V_m)^{1/2}$ for calculation of wind speed.

Figure 5. Values of Diffluence and Downwind Shear During Passage of the Extratropical Storm on 16 November 1983. Measurement by the GL radar in Sudbury, MA.
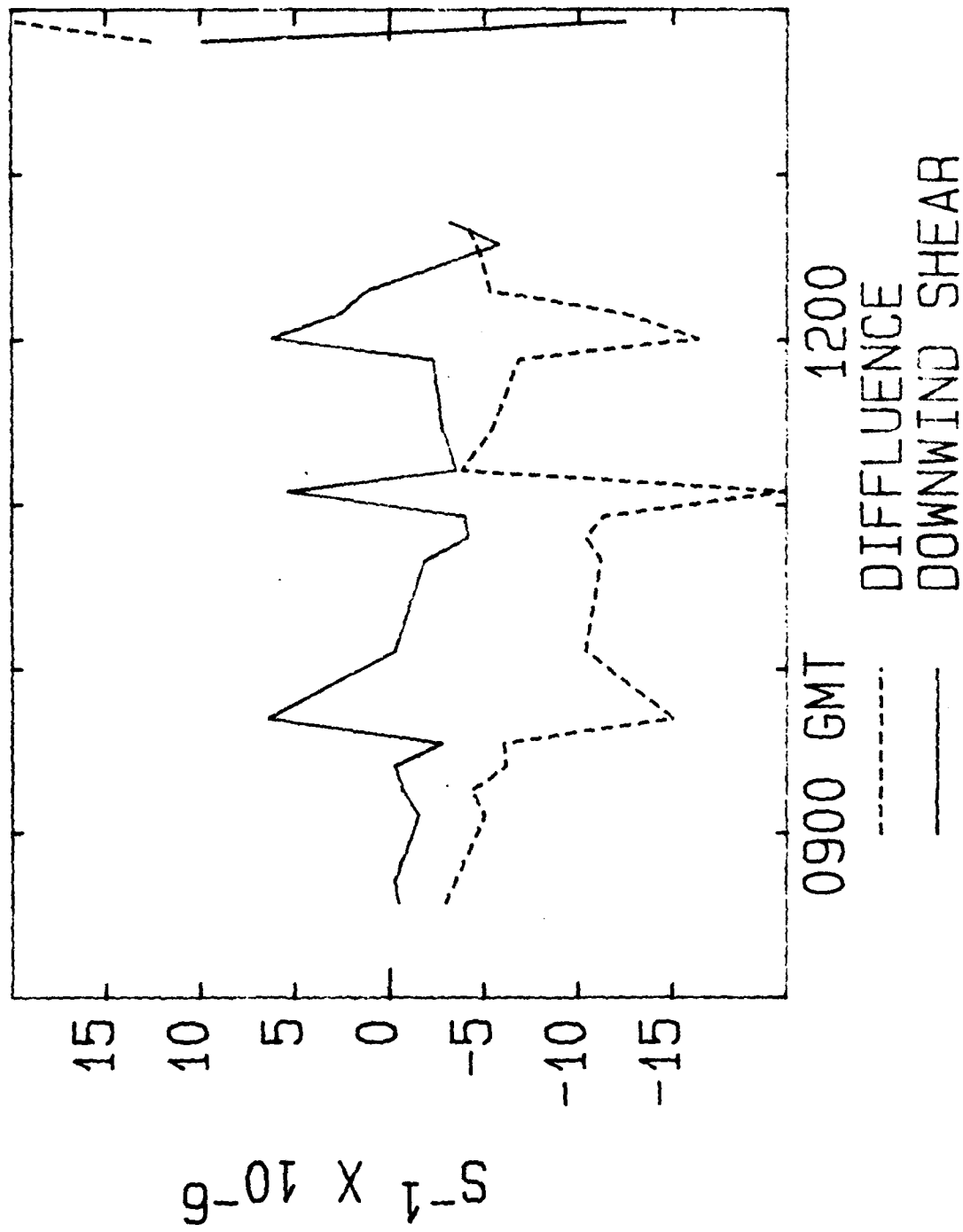
14

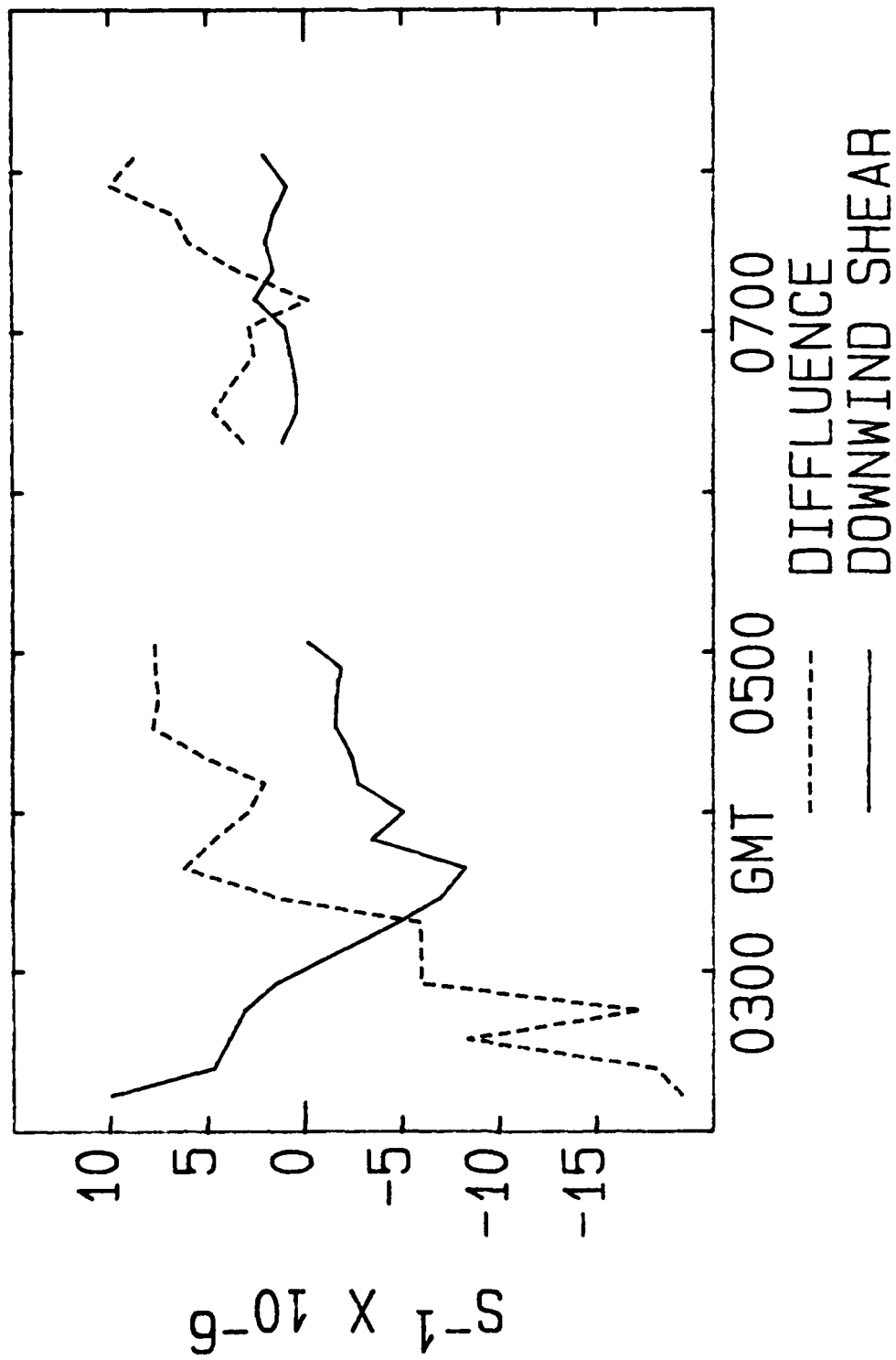Figure 6. Values of Diffluence and Downwind Shear During the Passage of the Extratropical Storm on 11 January 1984. Measurement by the GL radar in Sudbury, MA.
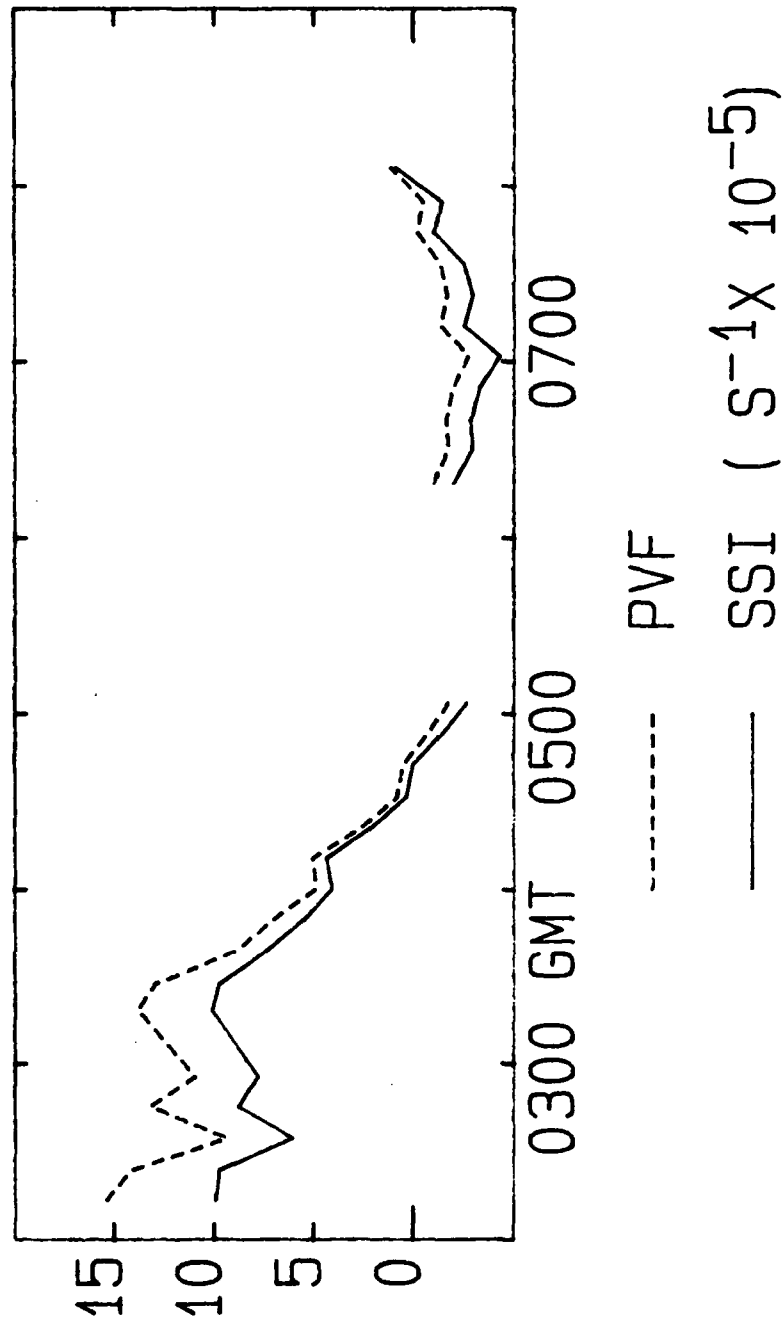
Figure 7. Values of Potential-Vortex Fit (PVF) and Storm Strength Index (SSI) during the passage of the Extratropical Storm on 11 January 1984. Measurement by the GL radar in Sudbury, MA.
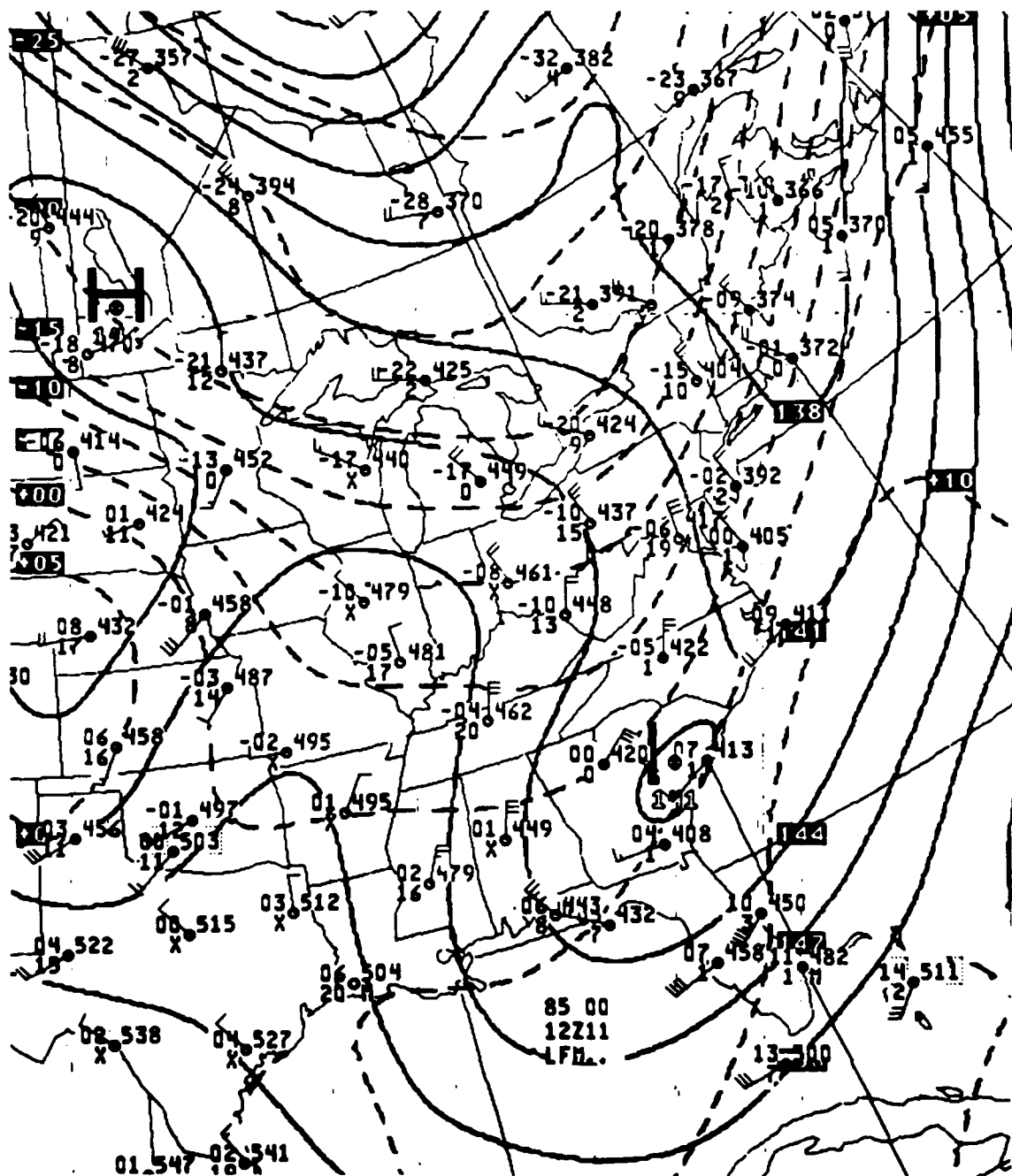
16

Figure 8. Analysis at 850 mb Level for 1200 GMT 11 January 1984

3.3 29 March 1984

On 29 March 1984 a very intense winter storm made its way up the Eastern Seaboard. At 0000 GMT the surface low was located over North and South Carolina with a central pressure of 980 mb. At this time the storm was responsible for very severe weather in the Carolinas including a series of deadly tornadoes. At 1200 GMT the storm was located over the Delmarva Peninsula and had deepened to 969 mb. From there the storm moved east-northeastward so that at 0000 GMT 30 March 1984 it was located 175 km south of Nantucket. The upper level support for this system appeared as cutoff lows at 850 mb, 700 mb, and 500 mb.

Because 29 March was during a hiatus of the Boston Area NEXRAD Demonstration, the radar operation began at approximately 1200 GMT and continued until 1730 GMT when a power failure halted measurements. Only the observations for the first hour contain enough data for the present analysis. After 1300 GMT the precipitation broke up into more convective type precipitation. Data from the second elevation step at 1.4° was used with a scanning circle of 40 km. The resultant height of 1182 meters was approximately that of the 850 mb level. A cutoff low at 850 mb was located just off the Maryland Eastern Shore approximately 640 km southwest of the radar site. Although we do not have enough data to provide a good history of the storm it is instructive to see what kind of values we get for the wind field derivatives and resultant indexes, especially the storm intensity indexes, since this storm was one of the strongest storms to make its way up the East Coast in many years. The average values for the five Velocity Area Display observations that were made between 1200 GMT and 1300 GMT 29 March 1984 are given in Table 7. The most noteworthy result is that PVF yields a

Table 7. Average values of the windfield derivatives and storm intensity indexes measured by the GL radar located in Sudbury, MA, for the period between 1200 GMT and 1300 GMT, 29 March 1984 for a scanning circle radius of 40 km at an elevation of 1.4°.

DIFFLUENCE	-1.721×10^{-6} s^{-1}
DOWNWIND SHEAR	6.559×10^{-6} s^{-1}
WIND SPEED	29.40 m s^{-1}
SSI	-1.164×10^{-5} s^{-1}
PVF	0.384

significantly higher value than SSI. This means that the crosswind shear is a function of distance to the storm center (closer to Potential Vortex flow) and not a constant, as assumed in the calculation of SSI.

3.4 12 February 1988

In the early evening of 11 February 1988 a low pressure system stretched from the Ohio Valley north to the lower Great Lakes. At this time a secondary low was present off the South Carolina coast. High pressure was located in Quebec. Throughout the evening into the next day both surface low pressure systems deepened with the original low moving north to be centered in the province of Ontario at 2100 GMT 12 February. By this time the coastal low had become the stronger of the two

18

centers and was located just to the south of Martha's Vineyard. The overall surface pattern was very complex with other weaker lows and fronts present. The upper air support for these surface systems was a trough located in the Midwest with closed circulation at 850 mb and 500 mb. The height of the cutoff low at 850 mb was at 1141 meters at 0000 GMT 12 February and had lowered to 1133 meters at 1200 GMT. There were no analyses available for 0000 GMT 13 February due to a computer shutdown at the National Meteorological Center.

Use of a scanning circle of 40 km at an elevation angle of 1.5° results in an effective height of 1251 m MSL which is approximately the height of the 850 mb level near the radar site. The values of SSI (Figure 9) were an order of magnitude lower than that found during Hurricane Gloria. Donaldson and Harris[6] state that an SSI < 10^{-4} s^{-1} indicates a less than vigorous storm. That may be true for tropical cyclones, but standards may have to be reduced when we examine extratropical cyclones and associated upper level systems. During the time the low at 850 mb moved from 614 km to 527 km relative to the radar site and during a period of deepening, the SSI reflects the increasing of the 850 mb low intensity. The wind speeds were also increasing, indicating the presence of positive crosswind shear.

Donaldson[9] believes that PVF values greater than 1 indicate a local wind anomaly. The persistence of the values above unity indicate that we are not seeing a short term perturbation or anomaly in the data of the VAD scanning circle. Instead, what we might be seeing is the influence of some mechanism that results in more curvature than what is associated with the closed circulation at 850 mb over the Great Lakes. Although there is no hint of this from the 850 mb analysis, after 1600 GMT, features were noted that resemble a vortex signature associated with a developing trough line (Ruggiero and Donaldson[10]). The high values of PVF may indeed be the first sign of the feature that was later observed directly.

Figure 10 depicts the values of diffluence and downwind shear during the period of observations. The most noteworthy features here are the combination of positive downwind shear and diffluence found between 0824 and 0923 GMT and negative downwind shear and confluence between 1538 and 1559. These conditions would not be expected if the air flow were confined to only horizontal components. Both of these features are probably due to the interaction of flow from other levels due to the so called "conveyor belts" that are found in extratropical cyclones.[11]

4. DISCUSSION

Despite the fact that on occasion extratropical cyclones produce Doppler velocity signatures similar to tropical cyclones, the present study indicates that this is not the norm for east coast extratropical cyclones. One reason is that relatively simple extratropical cyclones do not have precipitation around the entire storm. Usually the west side of a cyclone is relatively drier air and

10. Ruggiero, F.H. and Donaldson, R.J, Jr. (1989) Features resembling single Doppler vortex signatures observed in an extratropical cyclone, *Preprints, 24th Conf. Radar Meteorol.*, Meteorol. Soc., Boston.

11. Harrold, T.W. (1973) Mechanisms influencing the distribution of precipitation within baroclinic disturbances, *Quart. J. Roy. Meteorol.* **80**:174-181.
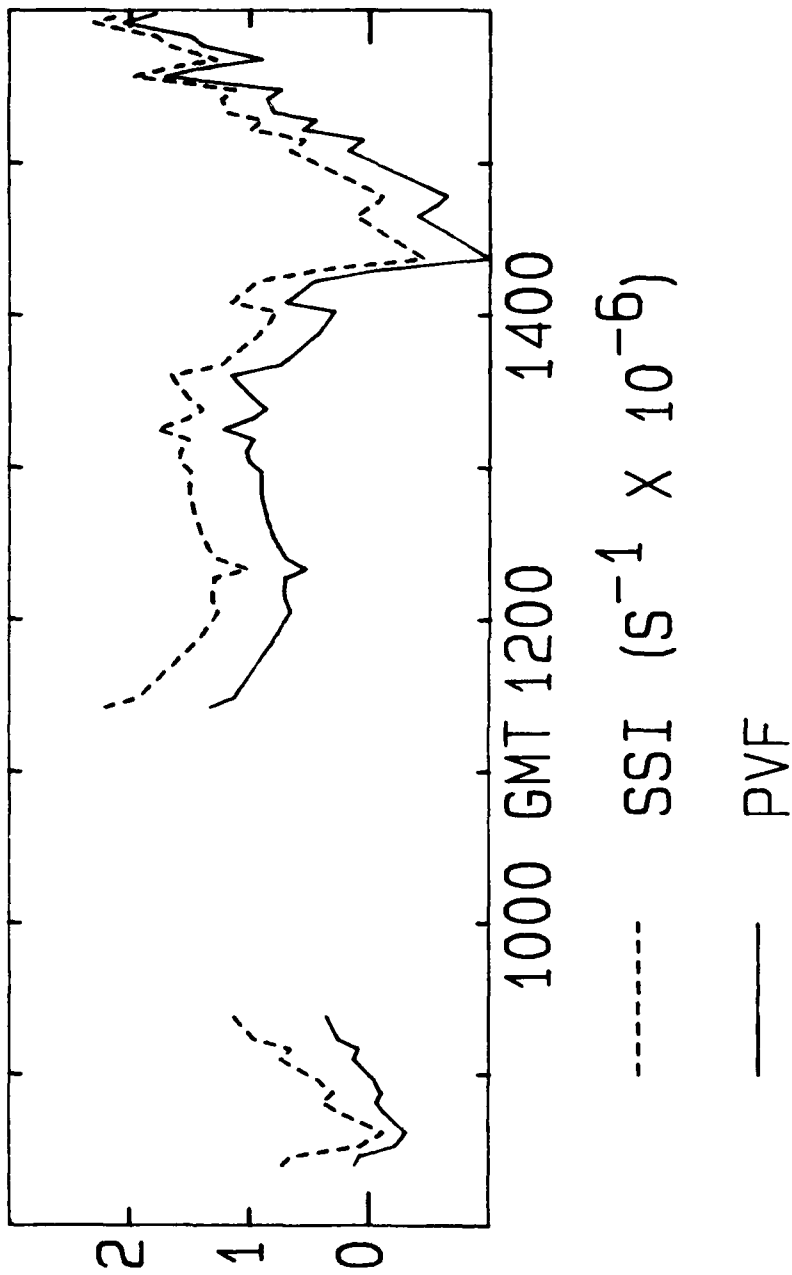
Figure 9. Values of Storm Strength Index (SSI) and Potential Vortex Fit (PVF) During the Passage of the Extratropical Storm on 12 February 1988. Measurement by the GL radar located in Sudbury, MA.
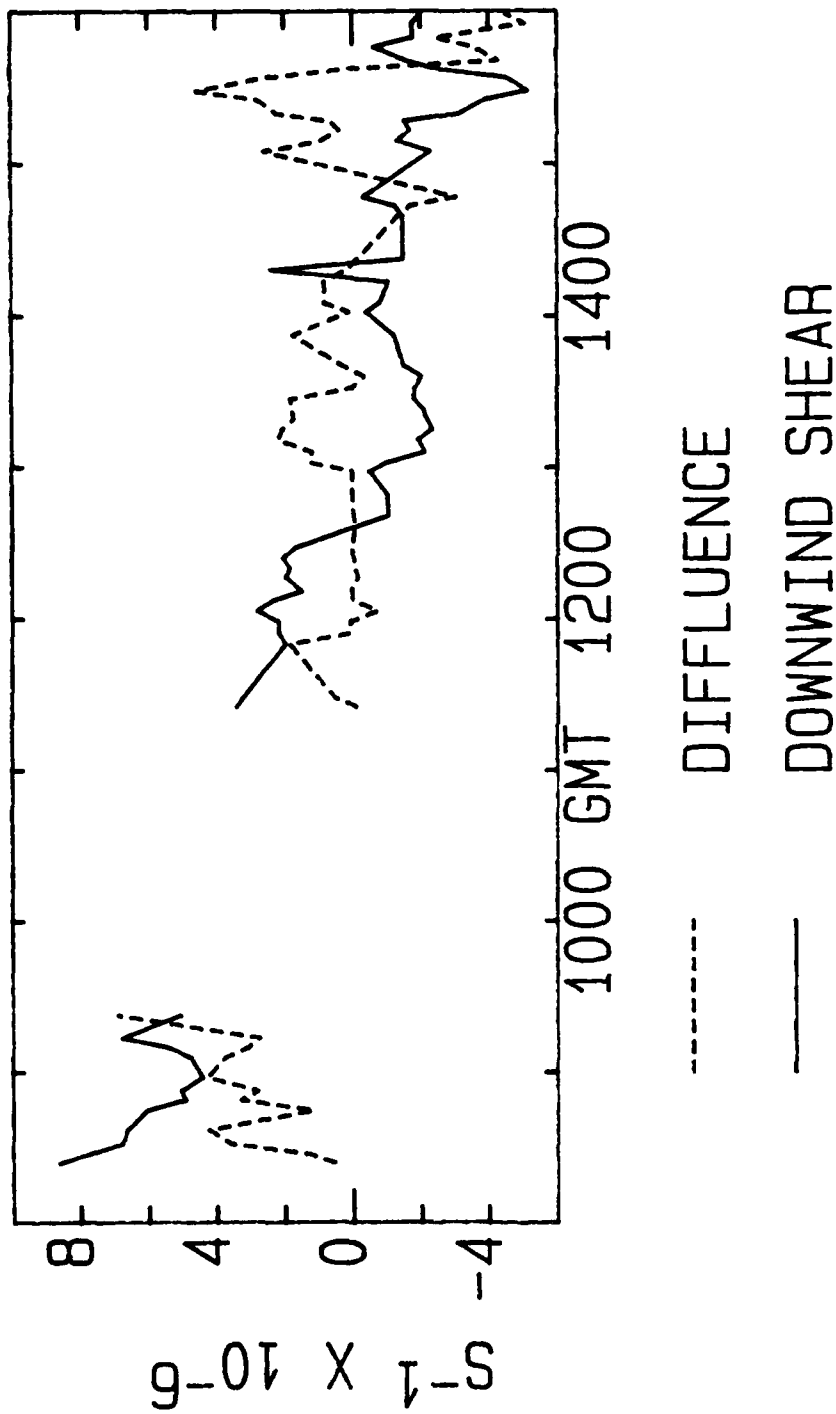
Figure 10. Values of Diffluence and Downwind Shear During the Passage of the Extratropical Storm on 12 February 1988. Measurement by the GL radar located in Sudbury, MA.

provides no radar echoes. The main stratiform precipitation area is just the northeast quadrant on the cool side of the associated warm front. Since we determined that we should work with VAD data that had 99 percent data coverage we eliminated a number of storms entirely as well as large amounts of time in storms we did analyze.

Another dissimilarity between extratropical cyclones and tropical cyclones is the amount of directional shear with height. Tropical cyclones tend to have vertically stacked closed circulation up to levels as high as 500 mb with perhaps some tilting present. Extratropical cyclones typically display much shear with height and include the tilting jets of wind that have been descriptively called "conveyor belts". The vertical shear causes two problems in the use of the wind field derivative analysis to quantify the strength of extratropical cyclones: 1) The conveyor belts lead to conditions of discontinuity by concurrently having positive downwind shear and diffluence and 2) The location of the principal circulation center at the surface may be drastically different from the location of the circulation at the height at which the scanning circle is located. Thus one is not sampling the storm itself, but one of the components contributing to the storm. In some of the cases discussed in this work it is obvious that when one looks at higher levels, where there are few closed circulations, the circulation of interest may not be the only contributor to the characteristics of the flow at that height.

Another factor that adds complexity to the use of wind field derivatives in extratropical cyclones is the exact positioning of the storm center when you do have enough data at a low elevation angle. In New England the particular problem with winter time extratropical cyclones is that they are generally comprised of two circulation centers, a primary low that moves eastward across the country and eventually gets hung up west of the Appalachian Mountains, and a secondary low that generally forms near the Atlantic coast. As with one of the cases descibed above, the surface analysis is some times even more complex than that. The problem is which low pressure center should be used as the circulation center to get an estimate of SSI and PVF. As shown above the solution has not yet been found.

5. CONCLUSIONS

As mentioned in the introduction it was hoped that by applying the technique of analyzing wind field derivatives in extratropical cyclones by Doppler radar we could get a better handle on forecasting these storms. While the estimations of the wind field derivatives of diffluence and downwind shear are credible since they do not rely on assumptions of the curvature parameter, it is presently unclear how to make use of the values in forecasting for extratropical storms. When the NEXRAD network is deployed, simultaneous readings of these derivatives from a number of radars might provide useful analysis and forecast information. The indexes SSI and PVF that are derived from a combination of crosswind shear and curvature have shown promise with tropical cyclones but do not work as well with the winter storms. The main problem is the unsuitability of the simple circulation model that is used for tropical cyclones when it is applied to extratropical cyclones.

References

1. Donaldson, R.J., Jr. and Harris, F.I. (1984) Detection of wind field curvature and wind speed gradients by a single Doppler radar, *Preprints, 22nd Conf. Radar Meteorol.*, Am. Meteorol. Soc., Boston, pp. 514-519.

2. Donaldson, R.J., Jr. and Ruggiero, F.H. (1986) Wind field derivatives in Hurricane Gloria estimated by Doppler radar, *Preprints, 23rd Conf. Radar Meteorol.*, Am. Meteorol. Soc., Boston, pp. 236-239.

3. Ruggiero, F.H. and Donaldson, R.J., Jr. (1987) Wind field derivatives: A new diagnostic tool for analysis of hurricanes by a single Doppler radar, *Preprints, 17th Conf. Hurricanes and Tropical Meteorol.*, Am. Meteorol. Soc., Boston, pp. 178-181.

4. Donaldson, R.J., Jr. (1989) Potential-vortex fit, *Preprints, 24th Conf. Radar Meteorol.*, Am. Meteorol. Soc., Boston.

5. Bosart, L.F. (1981) The Presidents' Day snowstorm of 18-19 February 1989: A subsynoptic-scale event, *Mon. Wea. Rev.* **109**:1542-1566.

6. U.S. Dept of Commerce (1984) *Storm Data*, NOAA, NESDIS, NCDC, Asheville, NC, 20 No. 2 (April) p. 4.

7. Donaldson, R.J., Jr. and Harris, F.I. (1989) On the determination of curvature, diffluence, and shear by Doppler radar, *J. Atmos. and Oceanic Tech.* **6**:26-35.

8. Browning, K.A. and Wexler, R. (1968) The determination of kinematic properties of a wind field using Doppler radar, *J. Appl. Meteorol.* **7**:105-113.

9. Forsyth, D.E., Istok, M.J., O'Bannon, T.D., and Glover, K.M. (1985) *The Boston Area NEXRAD Demonstration (BAND)*, AFGL-TR-85-0098, ADA164426.

10. Ruggiero, F.H. and Donaldson, R.J, Jr. (1989) Features resembling single Doppler vortex signatures observed in an extratropical cyclone, *Preprints, 24th Conf. Radar Meteorol.*, Meteorol. Soc., Boston.

11. Harrold, T.W. (1973) Mechanisms influencing the distribution of precipitation within baroclinic disturbances, *Quart. J. Roy. Meteorol.* **80**:174-181.

Appendix A

Interpolation Of The VAD Data

We start by determining the equation that we use to interpolate. We will use the equation for Fourier series extended to two orders:

$$V_p = a_0 + a_1\cos\alpha + b_1\sin\alpha + a_2\cos2\alpha + b_2\sin2\alpha \tag{A1}$$

where: V_p= the predicted velocity Doppler velocity based on using the above equation

a_0, a_1, b_1, a_2, b_2 = the Fourier coefficients

α = the azimuth angle

If we let V_m be the actual measured velocity then:

$$D = (V_m - V_p)^2 \tag{A2}$$

where D is the square of the deviation.
For all points:

$$\bar{D} = \frac{\Sigma(V_m - V_p)^2}{N} \tag{A3}$$

To minimize $\bar{D}$ we equate to zero the partial derivatives of $\bar{D}$ with respect to the coefficients:

$$\frac{\partial\bar{D}}{\partial a_0} = \frac{2}{N}\Sigma\left((V_m - V_p)\frac{\partial V_p}{\partial a_0}\right) = 0 \tag{A4}$$

$$\frac{\partial \bar{D}}{\partial a_1} = \frac{2}{N} \Sigma \left((V_m - V_p) \frac{\partial V_p}{\partial a_1} \right) = 0 \qquad \text{(A5)}$$

$$\frac{\partial \bar{D}}{\partial a_2} = \frac{2}{N} \Sigma \left((V_m - V_p) \frac{\partial V_p}{\partial a_2} \right) = 0 \qquad \text{(A6)}$$

$$\frac{\partial \bar{D}}{\partial b_1} = \frac{2}{N} \Sigma \left((V_m - V_p) \frac{\partial V_p}{\partial b_1} \right) = 0 \qquad \text{(A7)}$$

$$\frac{\partial \bar{D}}{\partial b_2} = \frac{2}{N} \Sigma \left((V_m - V_p) \frac{\partial V_p}{\partial b_2} \right) = 0 \qquad \text{(A8)}$$

Substituting for V_p and evaluating the partial derivative:

$$\frac{2}{N} \Sigma (V_m - a_0 - a_1 \cos\alpha - b_1 \sin\alpha - a_2 \cos2\alpha - b_2 \sin2\alpha) = 0 \qquad \text{(A9)}$$

$$\frac{2}{N} \Sigma [(V_m - a_0 - a_1 \cos\alpha - b_1 \sin\alpha - a_2 \cos2\alpha - b_2 \sin2\alpha) \cos\alpha] = 0 \qquad \text{(A10)}$$

$$\frac{2}{N} \Sigma [(V_m - a_0 - a_1 \cos\alpha - b_1 \sin\alpha - a_2 \cos2\alpha - b_2 \sin2\alpha) \cos2\alpha] = 0 \qquad \text{(A11)}$$

$$\frac{2}{N} \Sigma [(V_m - a_0 - a_1 \cos\alpha - b_1 \sin\alpha - a_2 \cos2\alpha - b_2 \sin2\alpha) \sin\alpha] = 0 \qquad \text{(A12)}$$

$$\frac{2}{N} \Sigma [(V_m - a_0 - a_1 \cos\alpha - b_1 \sin\alpha - a_2 \cos2\alpha - b_2 \sin2\alpha) \sin2\alpha] = 0 \qquad \text{(A13)}$$

The result is five unknowns in five equations. Reorganizing and changing into matrix notation we wind up with:

$$
\begin{vmatrix}
\Sigma 1 & \Sigma\cos\alpha & \Sigma\sin\alpha & \Sigma\cos2\alpha & \Sigma\sin2\alpha \\
\Sigma\cos\alpha & \Sigma\cos^2\alpha & \Sigma\sin\alpha\cos\alpha & \Sigma\cos2\alpha\cos\alpha & \Sigma\sin2\alpha\cos\alpha \\
\Sigma\sin\alpha & \Sigma\sin\alpha\cos\alpha & \Sigma\sin^2\alpha & \Sigma\cos2\alpha\sin\alpha & \Sigma\sin2\alpha\sin\alpha \\
\Sigma\cos2\alpha & \Sigma\cos2\alpha\cos\alpha & \Sigma\cos2\alpha\sin\alpha & \Sigma\cos^2 2\alpha & \Sigma\sin2\alpha\cos2\alpha \\
\Sigma\sin2\alpha & \Sigma\sin2\alpha\cos\alpha & \Sigma\sin2\alpha\sin\alpha & \Sigma\sin2\alpha\cos2\alpha & \Sigma\sin^2 2\alpha
\end{vmatrix}
\begin{vmatrix}
a_0 \\ a_1 \\ b_1 \\ a_2 \\ b_2
\end{vmatrix}
=
\begin{vmatrix}
\Sigma V_m \\ \Sigma V_m \cos\alpha \\ \Sigma V_m \sin\alpha \\ \Sigma V_m \cos2\alpha \\ \Sigma V_m \sin2\alpha
\end{vmatrix}
$$

which we solve for the Fourier coefficients.